Current Topics in Toxicology
Vol. 18, 2022

Original Article

Freshwater clam as a potential bioindicator for ZnO-agar nanocomposite toxicity

Tahani Younis Omar[1], Elizabeth Samir Sadek[2], Manar Ahmed Bahaaeldine[3], Aya Ramadan Rashed[3], Abdeljalil Mohamed Al Shawoush[3], Ayman S. Mohamed[3,*] and Dalia Y. Saad[3]

[1]Department of Zoology, Faculty of Science, Sirte University, Sirte, Libya.
[2]Faculty of Biotechnology, October University for Modern Sciences and Arts (MSA), Egypt;
[3]Zoology Department, Faculty of Science, Cairo University, Giza, Egypt.

ABSTRACT

ZnO nanoparticles (ZnO NPs) are widely used in medicine, food preservation, and other industres. The current study aims to evaluate the toxic effect of zinc oxide-agar nanocomposites on *Coelatura aegyptiaca* which is considered as a sensitive bioindicator for environmental pollution. Following the synthesis and characterization of zinc oxide nanoparticles (ZnO NPs) and ZnO-agar, different doses (12.5, 25, 50 mg/L) were tested. In addition to histology investigation, oxidative stress indicators were examined after seven days. ZnO NPs and ZnO-agar nanocomposite (NC) caused a significant increase in malonaldehyde and nitric oxide concentrations, while they decreased glutathione and catalase levels. Furthermore, bivalves treated with ZnO NPs and ZnO-agar NC showed structural alterations in their gills and mantle. In general, using agar in the synthesis of ZnO NPs results in synergistic effects such as cellular and structural damage and a more prominent alteration in biochemical parameters. In addition, we found that *Coelatura aegyptiaca* is an effective bioindicator for nanoparticle toxicity and water pollution.

KEYWORDS: clam, zinc oxide-agar nanocomposites, water pollution, toxicity, *Coelatura aegyptiaca*, histology, oxidative stress.

*Corresponding author: ayman81125@cu.edu.eg

1. INTRODUCTION

Nanomaterials were mixed with renewable and biodegradable polymers to generate unique and more effective materials that may replace the traditional materials [1]. Agar is a biopolymer extracted from red cell wall and is widely utilized in biomedical applications. Agar film is used as a common food packaging material due to its transparency, homogeneity, and flexibility [2]. In recent years, nanoparticles have gotten greater attention as the nanotechnology field has progressed. One of the most studied nanoparticles is zinc oxide nanoparticles (ZnO NPs). ZnO NPs have been widely explored in the medical field for their antibacterial, antioxidant, anticancer, antidiabetic and drug delivery properties [3].

In addition, the antibacterial activity of ZnO NPs has been researched for use in food packaging. Incorporating ZnO NPs in polymer composites to improve packaging properties has been investigated [4]. Because of the wide application of ZnO NPs, there is a greater danger of them being released into the environment. Environmental levels of ZnO NPs are predicted to continue to grow due to their widespread use. However, only a limited number of studies describe the ecotoxicological effects of ZnO NPs across all species [5]. The ZnO NP-mediated toxicity is demonstrated in many species, including microbes, bacteria, invertebrates, and vertebrates. Several investigations on freshwater

creatures, such as *Daphnia magna* and *Thamnocephalus platyurus*, have found that ZnO NPs are toxic [6]. Filter-feeding bivalves have been utilized as excellent models for studying NP toxicity.

Furthermore, freshwater clams like *Coelatura aegyptiaca* have the potential to accumulate trace metals from the surrounding aquatic environment in their tissues [7]. *Coelatura aegyptiaca* is a molluscan bivalve belonging to the Unionidae family that lives in Egypt's Nile river [8]. After exposure to various dosages of ZnO NPs, oxidative stress and the genotoxic impact was evaluated in *Coelatura aegyptiaca* [9]. However, there is no report on the toxicity of ZnO-agar NC. So, in the current study, we aim to evaluate the toxic effect of ZnO-agar NC using *Coelatura aegyptiaca* as a bioindicator to examine oxidative stress and histological alterations owing to the nanocomposite's toxicity.

2. MATERIALS AND METHODS

2.1. Materials

Zinc acetate dihydrate ($Zn(O_2CCH_3)_2(H_2O)_2$), sodium hydroxide (NaOH), agar, and all other reagents were purchased from Sigma-Aldrich (St. Louis, MO, USA), unless stated otherwise.

2.2. Synthesis of ZnO NPs

Synthesis of ZnO NPs was done according to Cao *et al*. [10]. In brief, 7.22 mmol of NaOH dissolved in 320 µL of bi-distilled water and then in 25 mL of ethanol was added dropwise to 3.73 mmol of zinc acetate dihydrate dissolved in 40 ml of ethanol, under vigorous and constant stirring for 2.25 h at 45, 50, 55, 60, and 65 °C, then the solution was allowed to cool down to room temperature. Then ZnO samples were collected by centrifugation and washed thoroughly with pure fresh ethanol repeatedly. ZnO NPs were re-dispersed in ethanol or dried at 60 °C for 2 h. All ZnO NPs were stored at room temperature.

2.3. Synthesis of ZnO-agar NC

Molten agar was prepared by dissolving 2.5 g of agar powder in 100 mL of dd H_2O in three separate beakers, which were heated at 90 °C for 1 hr with continuous stirring at 1000 rpm. 100 mg of ZnO NPs were added into agar, and samples were further heated and mixed at 90 °C for 30 min at 1000 rpm. 0.75 g of glycerol was added in the sample mixture as a plasticizer. The mixture was then heated till it became a sticky liquid, and immediately poured onto a glass Petri-dish. The sample was allowed to cool down at room temperature for 24 h, and then dried in an oven at 40 °C for 2 h. The prepared films were removed from glass plates and stored until further use [11].

2.4. Determination of ZnO concentration

ZnO concentrations were determined using ICP-OES equipment (iCAP 6500 Duo, Thermo Scientific, Cambridge, UK) at 213.856 nm. Before the measurement, sonication was performed for 20 minutes. The analyses were performed in triplicates.

2.5. Characterization of ZnO

Optical absorption of ZnO NPs and ZnO-agar NC was detected using a double beam UV-Vis spectrophotometer (Shimadzu UV-1601) at a wavelength range of 200–800 nm at room temperature.

The resulting powder was characterized by X-ray diffraction (XRD) pattern. The XRD pattern of ZnO NPs and ZnO-agar NC powder was acquired at room temperature with a panalytical X'PERT PRO X-ray diffractometer equipped with a Ni filter using Cu Kα radiations as X-ray source.

ZnO NPs and ZnO-agar NC structure was observed by transmission electron microscopy (FETEM, JEM-2100F, JEOL Inc., Japan) at an accelerating voltage of 200 kV.

2.6. Experimental animal

Freshwater bivalves, *Coelatura aegyptiaca*, were collected from the Nile River in Abu Rawash area, Giza Governorate, Egypt. The shell length was 12-15 cm and width 6-9 cm. An acclimatization phase lasting was 7 days in glass-reinforced plastic (FRP) tank at room temperature was required before the usage of the animals in the studies. The animals were fed with commercial phytoplankton during the experiment.

2.7. Experimental design

A stock suspension of 1000 mg/L ZnO-agar NC was prepared by dispersing ZnO-agar NC in dechlorinated

freshwater with incubation in an ultrasound bath for 90 minutes; another 20 minutes of sonication was performed directly before replacing the water every day. Exposure solutions were prepared immediately before use by diluting the stock solution in dechlorinated freshwater.

Three different doses of ZnO-agar NC as well as ZnO NPs (12.5, 25, and 50 mg/L) were selected in the present study. For each concentration, five bivalves were exposed to ZnO-agar NC or ZnO NPs for seven days. A parallel control set of bivalves was kept in clean dechlorinated freshwater. ZnO-agar NC and ZnO NPs dechlorinated freshwater solutions were changed daily, and their turbidity was measured before and after each water substitution to monitor exposure concentrations.

Using forceps, soft tissue was pulled out from the shell. The mantle, foot, hepatopancreas, and gills of each exposed bivalve were rapidly removed, and washed with ice-cold saline (0.9%), and the accessory connective fat tissue was cleaned.

The collected tissues (10% w/v) were homogenized in cold ice 0.1 M buffer Tris HCl (pH 7.4). The homogenate was centrifuged at 860 ×g for 10 min at 4^{o} C and the resultant supernatant was used for biochemical analysis [12, 13].

2.8. Oxidative stress markers

Oxidative stress markers were detected in the supernatant of the tissue homogenate. Biodiagnostic kits (Biodiagnostic Dokki, Giza, Egypt) were used for the determination of lipid peroxidation, which was measured by the formation of malondialdehyde (MDA) [14], glutathione (GSH) [15], catalase [16], and nitric oxide (NO) [17] using UV-Vis spectrophotometer (Shimadzu UV-1601).

2.9. Histopathological investigations

Tissue samples of the mantle and gills were dissected and fixed in 10% buffered formalin and then dehydrated in a graded series of ethanol, and finally immersed in xylene and embedded in paraffin wax (58–60 ˚C) using an automatic processor. Paraffin blocks were trimmed to suitable size and sections of tissues were cut at 5–6 μm thickness using a microtome (ModelRM2245, Leica Biosystems, Wetzlar, Germany). After deparaffinization, sections were rehydrated, stained with hematoxylin and eosin, mounted with Cristal/Mount, and subsequently subjected to pathological assessment [18, 19].

2.10. Statistical analysis

Reported values are represented as means ± SE. Statistical analysis was done by one-way analysis of variance (ANOVA) and Duncan post hoc test. Statistical analysis was performed using Statistical Processor System Support “SPSS” for Windows software. A value of $P < 0.05$ was considered significant.

3. RESULTS

3.1. ZnO concentration

For each exposure concentration, 50, 25, and 12.5 mg/L, the measured concentrations of ZnO in the ZnO-agar nanocomposite solution were 45.31, 21.75, and 9.027 mg/L, respectively (Fig. 1).

3.2. Characterization of ZnO

In the current investigation, ZnO NPs revealed a distinctive peak at 360 nm (Fig. 2A). The distinctive peak of ZnO-agar NC was seen at 290 nm (Fig. 2B).

In Fig. 3, ZnO NPs’ diffraction peaks were found in the range of angle (2θ) 20–80°, which revealed Bragg reflections with 2θ values of 31.84°, 34.52°, 36.33°, 47.63°, 56.71°, 62.96°, 68.13°, and 69.18° demonstrating the hexagonal type of ZnO NPs.

However, the diffraction peaks were found in the XRD analysis of ZnO-agar at 31.98°, 34.66°, 36.81°, 47.71°, 56.83°, 63.12°, 65.51°, and 68.32° (Fig. 4). The obtained peaks confirmed the crystalline nature of the synthesized ZnO-agar NC.

ZnO nanoparticles were aggregated and comprised of polygonal nanostructures with smooth surfaces and an inner size of 3-5 nm, according to TEM images of the synthesized ZnO NPs (Fig. 5).

On the other hand, TEM examination revealed that synthesized ZnO-agar NC had a spherical form, a smooth surface, and an average size of 26.5 nm (Fig. 6).

3.3. Oxidative stress markers

MDA levels were significantly elevated ($P<0.05$) in ZnO NPs and ZnO-agar NC-treated tissues (mantle, gills, foot, digestive gland) in a dose-dependent manner when compared to the control group (Table 1). Despite this, bivalves treated

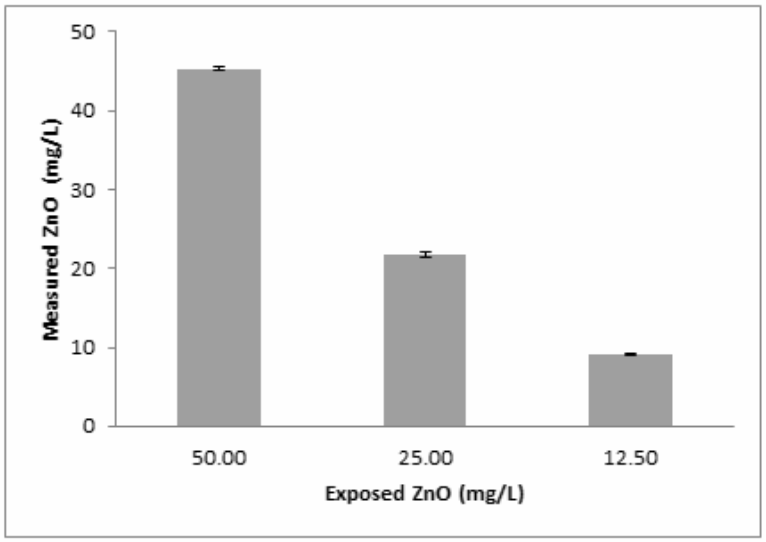

Fig. 1. ZnO concentration in ZnO-agar NC (n = 3 for each concentration).

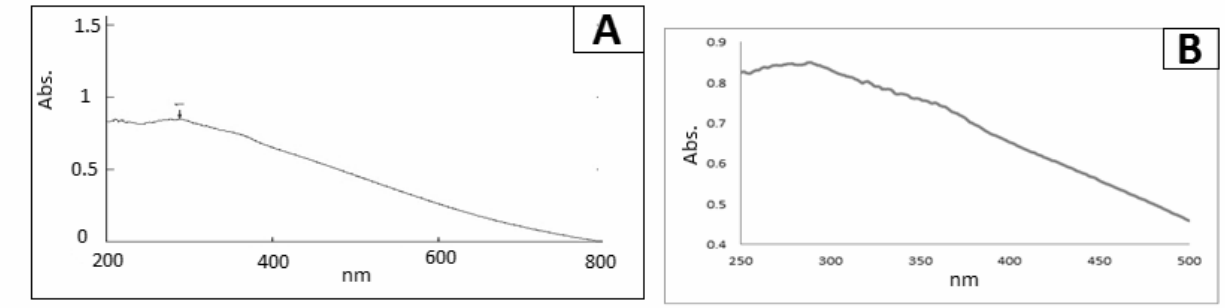

Fig. 2. UV–Visible absorption spectrum of ZnO NPs (**A**) and ZnO-agar NC (**B**).

with the lowest concentration of ZnO NPs in their mantle showed no significant change ($P>0.05$) in their MDA levels.

In our research, all four tissues evaluated showed a significant decrease ($P<0.05$) in GSH level in a concentration-dependent manner after exposure to various dosages of ZnO NPs and ZnO-agar NC (Table 2).

In treated bivalves of all tested concentrations of ZnO NPs and ZnO-agar NC, catalase (CAT) activity significantly decreased ($P<0.05$) in a concentration-dependent manner as compared to controls (Table 3).

Compared to the control group, exposure of *Coelatura aegyptiaca* to various dosages of ZnO NPs and ZnO-agar NC increased NO values in all treated organisms (Table 4).

3.4. Histology of gills

In the present study, a histological examination of gills and mantle of the treated and untreated organisms was done (Fig. 7). Untreated gill tissue has a well-defined structure, with ciliated filaments that are frequently interrupted by ostia. A thin layer of flattened cells forms the water tube walls, which can sometimes include the elliptical hemolymph channel. Normal gills are made up of two gill lamellae, the inner and outer lamellae, with filaments running vertically along the lamellar surface. Septa, which are made up of a simple columnar epithelium and underlying fibrous connective tissue, connect the inner and outer lamellae. The epithelial layer and vascular system of each gill filament are coated with lateral

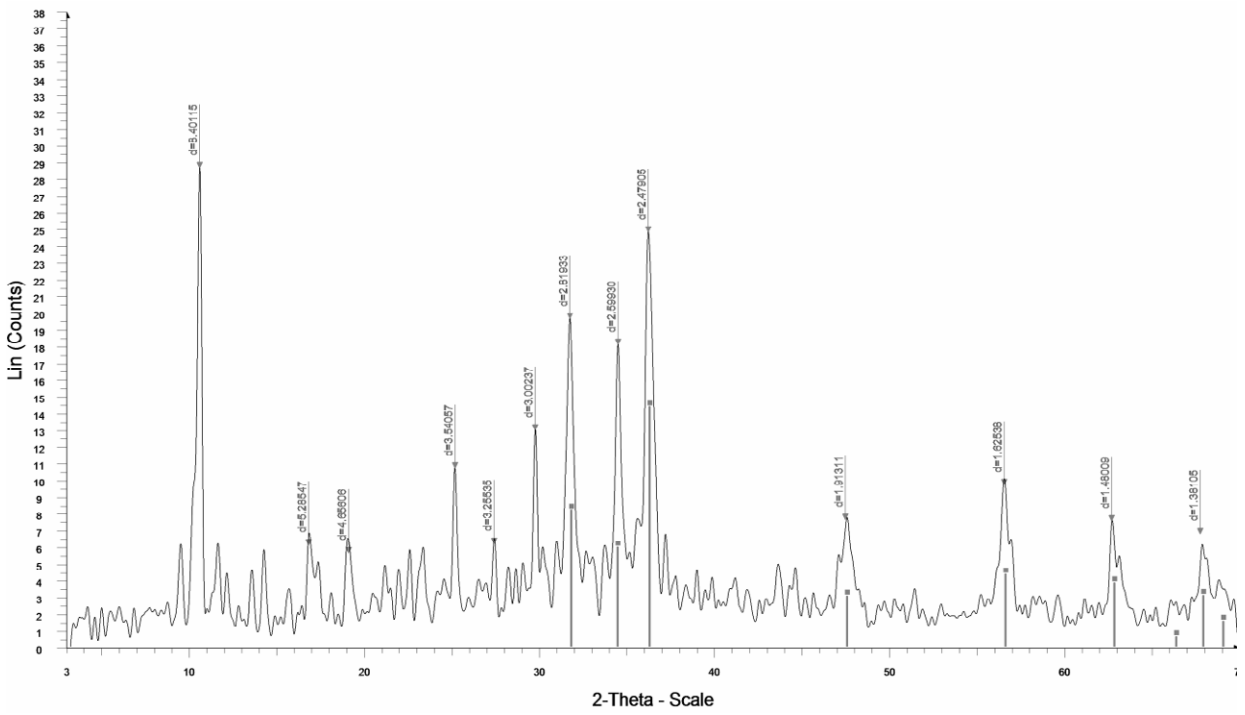

Fig. 3. X-ray diffractometer (XRD) analysis of ZnO NPs.

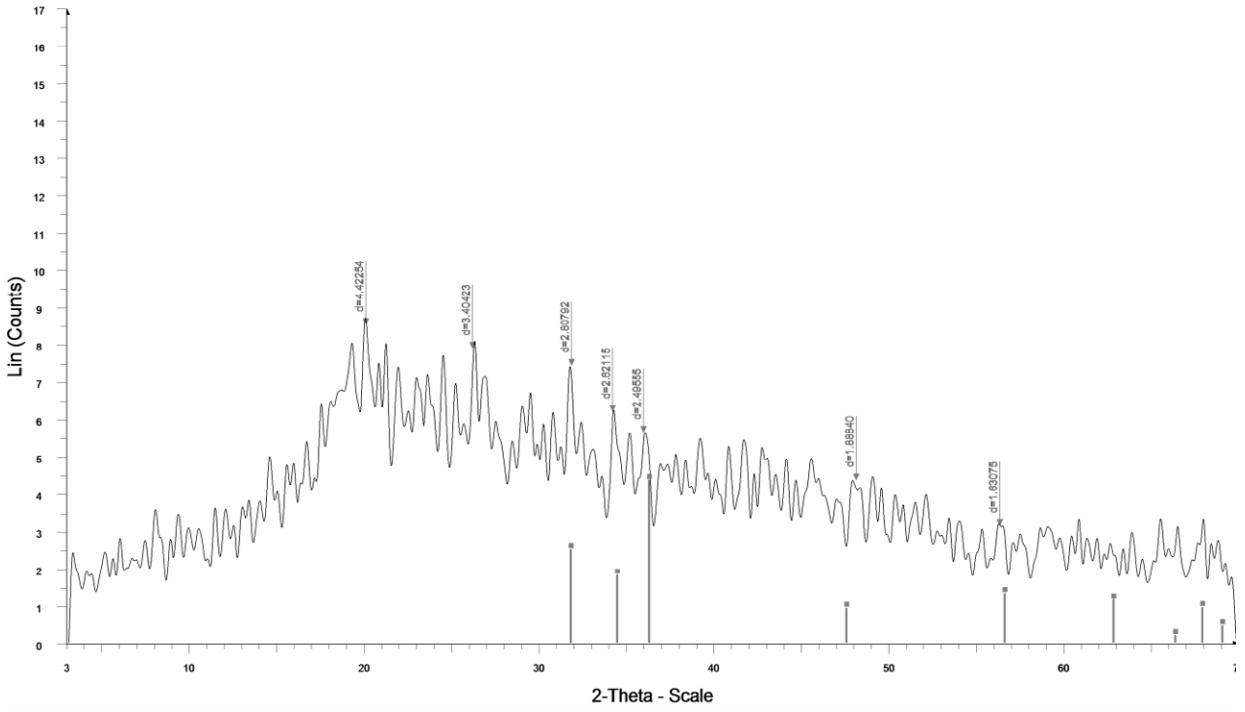

Fig. 4. X-ray diffractometer (XRD) analysis of ZnO-agar NC.

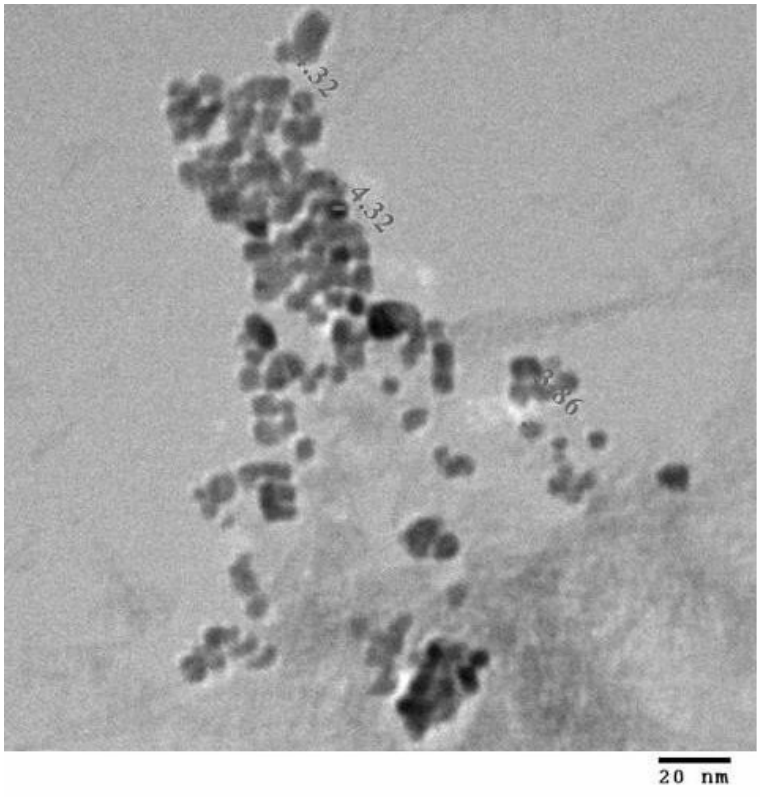

Fig. 5. TEM micrographs of ZnO NPs.

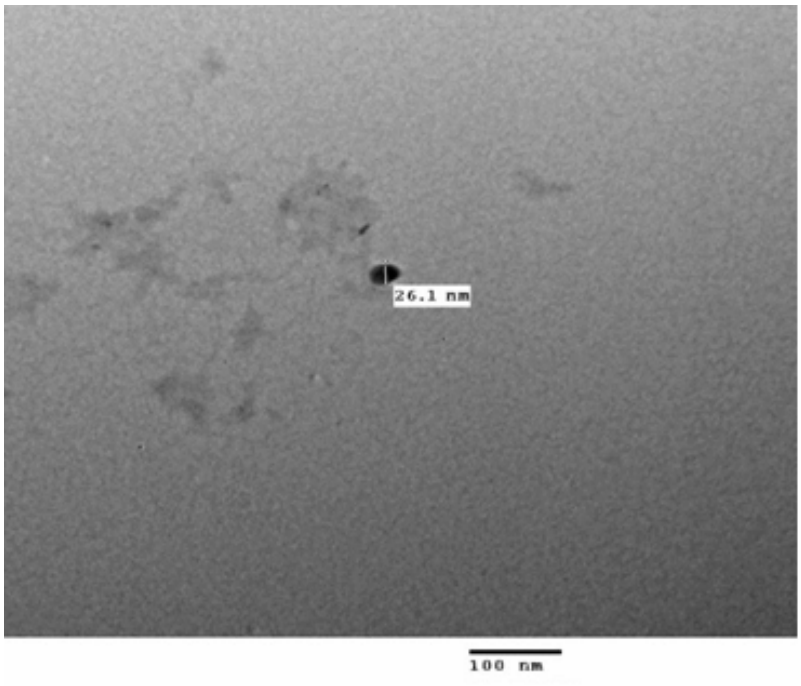

Fig. 6. TEM micrographs of ZnO-agar NC.

Table 1. Effect of ZnO NP and ZnO-agar NC concentrations on MDA (nmole/g. tissue) level in different organs of *Coelatura aegyptiaca*.

Concentrations		Organ			
		Mantle	**Gills**	**Digestive gland**	**Foot**
Control	**0**	0.71 ±0.04^{a}	0.94±0.08^{a}	0.58±0.04^{a}	0.33±0.02^{a}
ZnO NPs	**12.5 mg/L**	0.84 ±0.05^{a}	1.63±0.06^{b}	1.85±0.07^{b}	0.69±0.01^{b}
	25 mg/L	1.27± 0.03^{c}	2.00±0.08^{c}	2.32±0.06^{c}	0.81±0.02^{c}
	50 mg/L	1.50 ± 0.03^{d}	2.60±0.06^{d}	2.78±0.03^{d}	1.07±0.02^{d}
ZnO-agar NCs	**12.5 mg/L**	1.02 ± 0.04^{b}	2.09±0.08^{c}	3.16±0.11^{e}	0.70±0.02^{b}
	25 mg/L	1.45 ± 0.03^{d}	2.60±0.07^{d}	4.25±0.08^{f}	0.85±0.02^{c}
	50 mg/L	1.72 ± 0.02^{e}	3.03±0.08^{e}	4.71±0.06^{g}	1.31±0.07^{e}

Values are means ± SE (n = 5 per group). Values with different superscripted letters are significantly different (P <0.05).

Table 2. Effect of ZnO NP and ZnO-agar NC concentrations on GSH (mmole/g. tissue) level in different organs of *Coelatura aegyptiaca*.

Concentrations		Organ			
		Mantle	**Gills**	**Digestive gland**	**Foot**
Control	**0**	3.45 ±0.15 ^{f}	3.72±0.06^{e}	4.73±0.12^{f}	2.93±0.11^{e}
ZnO NPs	**12.5 mg/L**	2.70 ± 0.08 ^{e}	3.26±0.12^{d}	3.62±0.16^{e}	2.66±0.07^{d}
	25 mg/L	2.40±0.03^{d}	2.61±0.11^{c}	2.65±0.08^{d}	2.27±0.08^{c}
	50 mg/L	2.02±0.06^{c}	2.09±0.05^{b}	2.22±0.06^{c}	2.05±0.06^{b,c}
ZnO-agar NCs	**12.5 mg/L**	1.58±0.12^{b}	2.64±0.04^{c}	2.37±0.13^{c,d}	2.21±0.10^{b,c}
	25 mg/L	1.32±0.05^{a,b}	2.19±0.06^{b}	1.83±0.06^{b}	1.94±0.10^{b}
	50 mg/L	1.28±0.06^{a}	1.79±0.03^{a}	1.41±0.07^{a}	1.60±0.04^{a}

Values are means ± SE (n = 5 per group). Values with different superscripted letters are significantly different (P <0.05).

Table 3. Effect of ZnO NP and ZnO-agar NC concentrations on CAT (U/g. tissue) activity in different organs of *Coelatura aegyptiaca*.

Concentrations		Organ			
		Mantle	**Gills**	**Digestive gland**	**Foot**
Control	**0**	11.93±0.99^{f}	20.89±1.55^{e}	16.08±0.58^{e}	15.42±0.41^{e}
ZnO NPs	**12.5 mg/L**	6.82±0.20^{e}	14.04±0.65^{d}	11.02±0.73^{d}	10.09±0.48^{d}
	25 mg/L	3.91±0.11^{d}	9.46±0.88^{c}	8.66±0.33^{c}	7.07±0.07^{c}
	50 mg/L	3.56±0.16^{c}	5.04±0.18^{a}	5.74±0.20^{b}	5.27±0.15^{b}
ZnO-agar NCs	**12.5 mg/L**	3.18±0.09^{b}	9.21±0.16^{c}	5.29±0.22^{b}	6.97±0.02^{c}
	25 mg/L	2.44±0.11^{a,b}	7.33±0.33^{b}	3.81±0.26^{a}	3.49±0.04^{a}
	50 mg/L	2.22±0.07^{a}	3.67±0.26^{a}	2.91±0.22^{a}	2.87±0.04^{a}

Values are means ± SE (n = 5 per group). Values with different superscripted letters are significantly different (P <0.05).

Table 4. Effect of ZnO NP and ZnO-agar NC concentrations on NO (μmole/g. tissue) level in different organs of *Coelatura aegyptiaca*.

Concentrations		Organ			
		Mantle	**Gills**	**Digestive gland**	**Foot**
Control	**0**	7.51 ± 0.38^{a}	6.32 ± 0.36^{a}	4.2 ± 0.24^{a}	7.12 ± 0.23^{a}
ZnO NPs	**12.5 mg/L**	9.69 ± 0.58^{b}	10.36 ± 0.29^{b}	6.16 ± 0.47^{b}	13.94 ± 0.43^{b}
	25 mg/L	16.96 ± 0.34^{d}	15.05 ± 0.54^{c}	10.66 ± 0.62^{d}	14.30 ± 0.21^{b}
	50 mg/L	24.58 ± 0.35^{f}	22.58 ± 0.94^{d}	15.31 ± 0.47^{e}	16.24 ± 0.40^{c}
ZnO-agar NCs	**12.5 mg/L**	12.46 ± 0.56^{c}	11.64 ± 0.39^{b}	5.84 ± 0.19^{b}	17.28 ± 0.42^{c}
	25 mg/L	20.97 ± 0.44^{e}	16.34 ± 1.46^{c}	9.17 ± 0.13^{c}	18.01 ± 0.41^{c}
	50 mg/L	31.74 ± 0.76^{g}	25.02 ± 0.46^{e}	14.57 ± 0.31^{e}	18.25 ± 0.41^{c}

Values are means ± SE (n = 5 per group). Values with different superscripted letters are significantly different ($P < 0.05$).

and frontal cilia. Moreover, the filament's end was held by two chitinous plates found under the epithelium. Following exposure to 12.5 mg/L ZnO NPs for seven days, gill filaments showed a dilation in blood cells and breaking in lateral cilia. That was also observed in 12.5 mg/L ZnO-agar NC-exposed group. In Fig. 7 after exposure to 25 mg/L ZnO NPs, the frontal end of the gill filament was flattened, and there were less blood cells in the lumen. Furthermore, the frontal cilia were removed, while the lateral cilia were shortened. However, in 25 mg/L ZnO-agar NC-treated group, there were alterations in the filament structure and a decrease in the frontal cilia. The concentration of 50 mg/L of ZnO NPs caused haematocyte damage, disoriented chitinous rods, as well as shaded frontal cilia in the gills. In addition, in 50 mg/L ZnO-agarNC-treated bivalves, epithelial cell proliferation, lamellar fusion, blood cell expansion, and filament deregulation were also observed.

3.5. Histology of mantle

In light micrographs of the mantle, a plicated integument (PI), which represents the epithelium layer, a connective tissue layer containing granulocytes (GC) was observed (Fig. 8). In addition, a somatic musculature (SM) layer was seen in normal tissue. Ciliated columnar epithelial cells (CEC) and mucous cells made up the plicated integument. The longitudinal and cross-sections of myocytes were visible in the musculature layer of the mantle. Fig. 8 shows mild damage in the epithelial layer of the mussel's mantle after exposure to 12.5 mg/L ZnO NPs and ZnO-agar NC. However, both doses of ZnO NPs and ZnO-agar NC, 25 mg/L elicit severe degenerative alterations in the mantle, including muscle bundle breaking, severe muscular atrophy, and granulocytes enlargement. Despite being observed for both substances, the effect was more pronounced in tissues treated with ZnO-agar NC.

4. DISCUSSION

Nowadays, the toxicity of nanoparticles is a growing problem across the world because of its adverse effects on aquatic life, human health, as well as the whole ecosystem [20]. However, because of the positive aspects of nanoparticles in many fields and applications, it is also important to keep track of their negative effects. One of the recently used compounds is ZnO-agar NC. In our study, we aim to shed light on ZnO-agar NC's toxicity, illustrating its oxidative stress and histological effects on freshwater clam.

Using bivalves as a bioindicator, a great number of studies have successfully described metal toxicity, bioavailability, and bioaccumulation. Accumulated trace substances in bivalves can cause inability of cellular defense system to respond to elevated levels of free radicals which results in oxidative stress and tissue damage [21]. Several *in vitro* and *in vivo* studies have shown that metal oxide nanoparticles generate reactive oxygen species (ROS) and cause oxidative stress in cells and tissue [22].

Malonaldehyde (MDA) is a lipid peroxidation (LP) biomarker [23]. The increase in MDA level

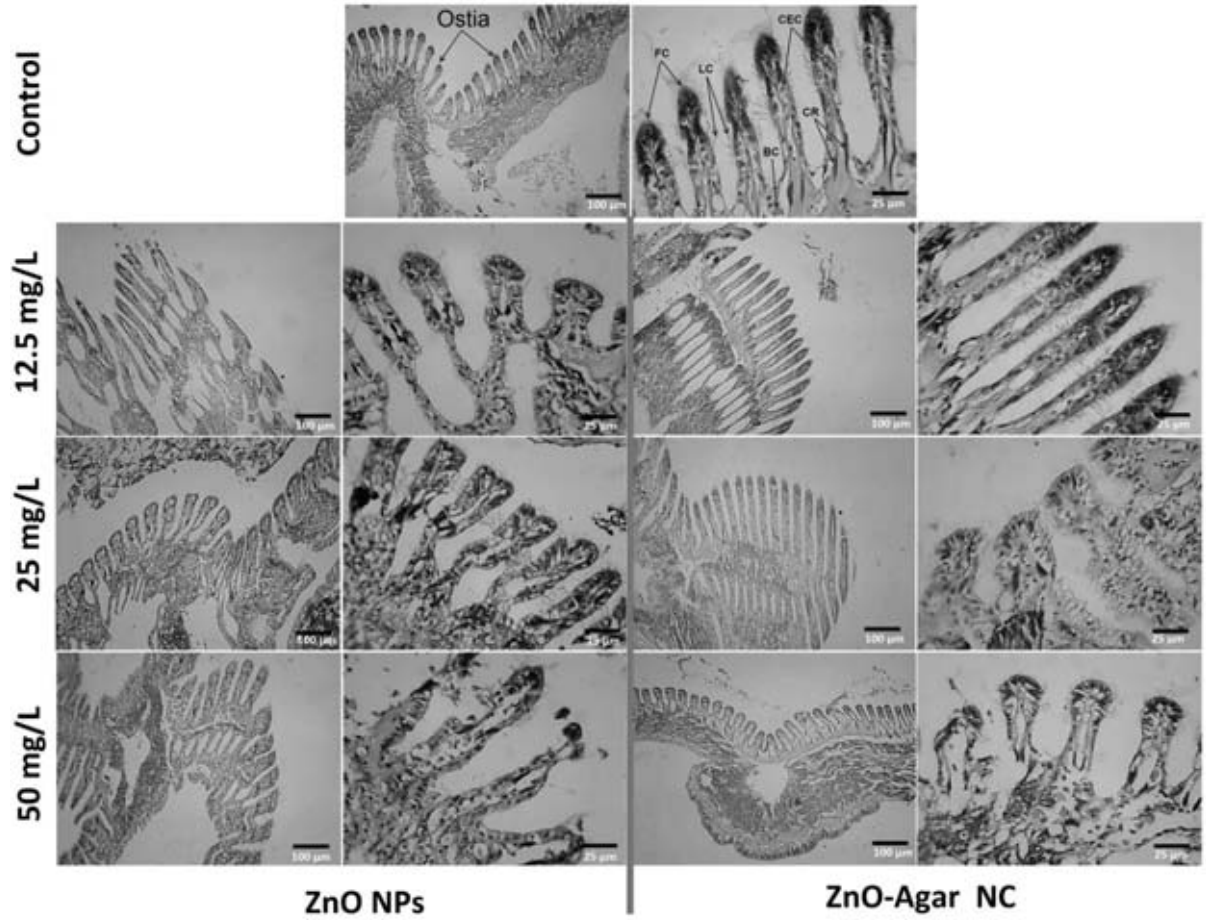

Fig. 7. Light micrographs of gills of *Coelatura aegyptiaca* exposed to ZnO NPs and ZnO-agar NC (100&400X H&E). "BC" blood cells, "CEC" ciliated columnar epithelial cells, "CR" chitinous rods. "FC" frontal cilia, and "LC" lateral cilia.

in the current study may be a result of overwhelming ROS production, which causes damage to cellular macromolecules [24]. Owing to the toxicity of NPs, the imbalance between free radicals and antioxidant enzymes leads to oxidative stress, increased LP production, and cell apoptosis. MDA is a by-product of LP that is widely employed as a marker for cell membrane damage [25].

On the other hand, glutathione reduced (GSH) a strong free-radical scavenger, is a tripeptide with antioxidant effects. As a result, GSH is a crucial component of the intracellular protective system against oxidative stress [26]. In our study, exposure to various doses of ZnO NPs and ZnO-agar NC caused decrease in GSH concentration. Our results agree with those of Mohamed *et al.* who indicated decreased levels of GSH after exposure to NPs. The reduced levels of GSH is a response to NP-triggered free radicals that convert GSH into its oxidized form glutathione [27].

One of the ROS-deactivating pathways is mediated by catalase (CAT). CAT is a large antioxidant enzyme that is responsible for the catalytic decomposition of hydrogen peroxide (H_2O_2) to water (H_2O) and molecular oxygen (O_2) following superoxide dismutation reaction [28]. Our result showed that CAT activity decreased in ZnO NPs and ZnO-agar NC groups. Similarly, *Coelatura aegyptiaca* infected with ZnO NPs exhibited inhibition of CAT activity.

The nitric oxide synthase (NOS), which catalyzes the conversion of L-arginine to L-citrulline and NO in invertebrates, is a critical enzyme in the production of nitric oxide (NO). NO is a putative regulator of bivalve metamorphosis, generated by

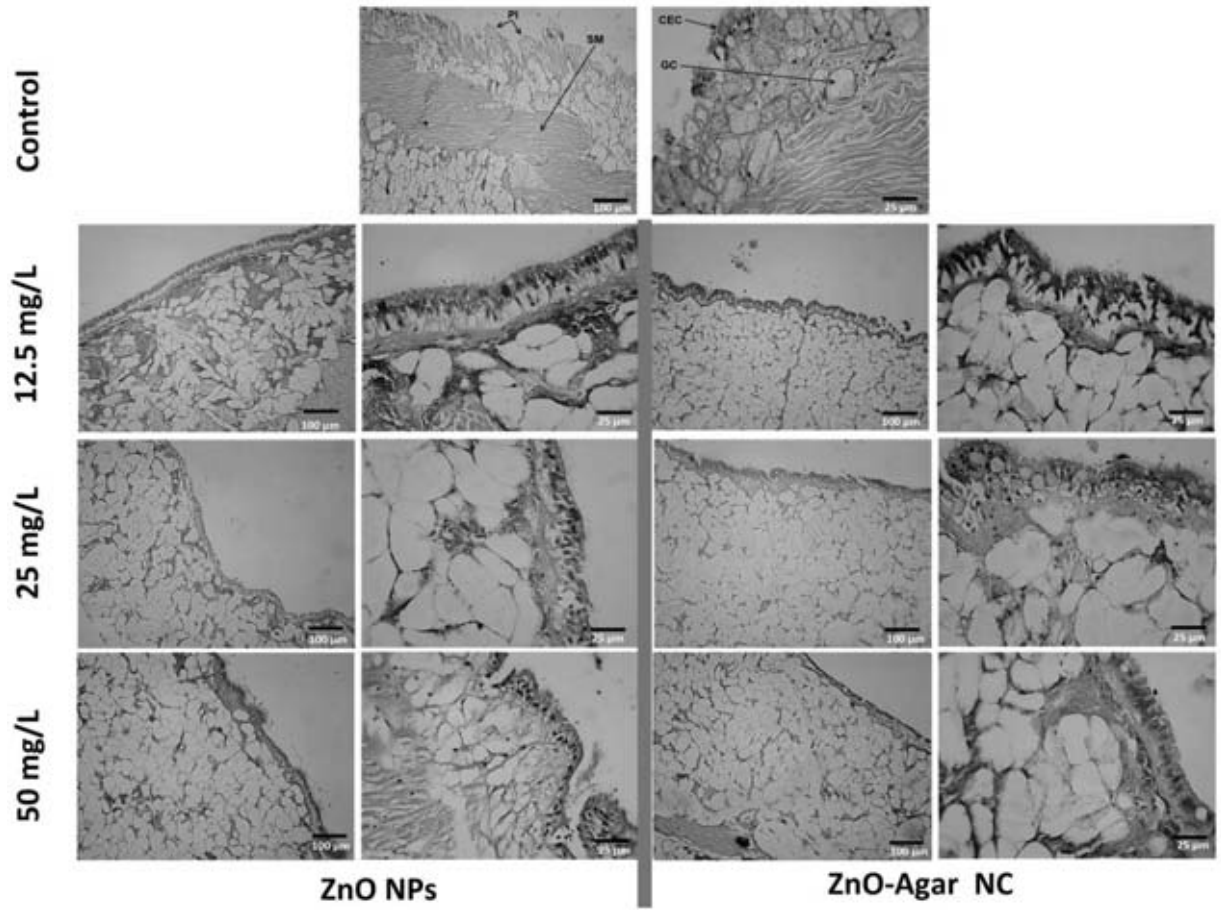

Fig. 8. Light micrographs of the mantle of *Coelatura aegyptiaca* exposed to ZnO NPs and ZnO-agar NC (100 & 400X H&E). "GC" granulocytes, "CEC" ciliated columnar epithelial cells, "SM" somatic musculature, and "PI" plicated integument.

mussel hemocytes [29]. Exposure of *Coelatura aegyptiaca* to various doses of ZnO NPs and ZnO-agar NC caused an elevation in NO level. Our outcomes are consistent with those of Canesi *et al.* [30], which suggests that metal NPs caused decreased phagocytic activity, increased lysozyme activity, oxidative stress, and NO production in a dose-dependent manner, triggering pre-apoptotic mechanism.

In general, using agar in the synthesis of ZnO NPs results in synergistic toxic effects, such as cellular and structural damage, and a more prominent alteration in the biochemical parameters measured.

5. CONCLUSION

In conclusion, exposure to ZnO nanoparticles and ZnO-agar nanocomposites generated an oxidative stress response in *Coelatura aegyptiaca*, as well as histological alterations in treated gills and mantle. As a result, we proposed that *Coelatura aegyptiaca* is an effective bioindicator for detecting any water contamination by nanoparticles.

ACKNOWLEDGEMENTS

The authors extend their appreciation to the Deanship of Scientific Research Cairo University, Egypt for supporting the current work.

CONFLICT OF INTEREST STATEMENT

None of the authors have any known competing financial interests or personal relationships that could have appeared to influence the work reported in this paper.

REFERENCES

1. Makwana, D., Castaño, J., Somani, S. and Bajaj, C. 2020, Arab. J. Chem,. 13(1), 3092-3099.

2. Mostafavi, F. S. and Zaeim, D. 2020, Int. J. Biol. Macromol., 159, 1165-1176.
3. Canaparo, R., Foglietta, F., Limongi, T. and Serpe, L. 2020, Materials, 14(1), 53.
4. Espitia, P. J. P., Coimbra,. S. D. R., Soares, N. F. F., de Andrade, N. J., Cruz, R. S. and Medeiros, E. A. A. 2012, Food Bioproc. Tech., 5(5), 1447-1464.
5. Ma, H., Williams, P. L. and Diamond, S. A. 2013, Environ. Pollut., 172, 76-85.
6. Zhang, W., Bao, S. and Fang, T. 2016, Sci. Rep., 6(1), 24839.
7. El Assal, F. M. and Sabet, S. F. 2014, Int. J. Waste Resour., 04(04), 1000163.
8. Mohamed, A. S., Ibrahim, W. M., Zaki, N. I., Ali, B. and Soliman, A. M. 2019, eCAM., 2019, 1-9.
9. Fahmy, S. R. and Sayed, D. A. 2017, Toxicol. Ind. Health., 33(7), 564-575.
10. Cao, D., Gong, S., Shu, X., Zhu, D., Liang, S. 2019, Nanoscale Res. Lett., 14(1), 210.
11. Kumar, S., Boro,. C., Ray, D., Mukherjee, A. and Dutta, J. 2019, Heliyon, 5(6), e01867.
12. Mohamed, A. S., Elkareem, M. A. M., Soliman, A. M. and Fahmy, S. R. 2022, Biointerface Res. Appl. Chem., 12(6), 7741-7751.
13. Youssef, A., Baiomy, A., Fahmy, S. R., Mohamed, A. S., Saad, D. and Desoky, R. 2022, Pharm. Sci. Asia., 49(2), 138-146.
14. Mamdouh, S., Mohamed, A. S., Mohamed, H. A. and Fahmy, W. S. 2021, Biol. Trace Elem., 200(1), 375-384.
15. Beutler, E., Duron, O. and Kelly, B. M. 1963, J. Lab. Clin. Med., 61, 882-888.
16. Aebi, H. 1984, Methods in Enzymology, Academic Press, UK.
17. Montgomery, H. and Dymock, J. 1961, Analyst., 86, 414-416.
18. Madany, N. M. K., Shehata, M. R. and Mohamed, A. S. 2022, Biointerface Res. Appl. Chem., 12(6), 8152-8162.
19. Magdy, A., Fahmy, S. R., Mohamed, A. S., Saad, D. Y., Desoky, R. S. and Baiomy, A. A. 2022, Int. J. Morphol., 40(1), 277-286.
20. Khan, I., Saeed, K. and Khan, I. 2019, Arab. J. Chem., 12(7), 908-931.
21. Strehse, J. S. and Maser, E. 2020, Mar. Environ. Res., 158, 105006.
22. Jayaram, D. T., Runa, S., Kemp, M. L. and Payne, C. K. 2017, Nanoscale, 9(22), 7595-7601.
23. Bahaaeldine, M. A., El Garhy, M., Fahm, S. R. and Mohamed, A. S. 2022, J. Parasit. Dis, 2022, 50-58.
24. Zhou, W., Tang, Y., Du, X., Han, Y., Shi, W., Sun, S., Zhang, W., Zheng, H. and Liu, G.2021, Mar. Pollut. Bull. 164, 111995.
25. Noshin, F., Ali, R. and Banik, S. 2021, J. Trace. Elem. Med. Biol., 64, 126707.
26. Witt, B., Stiboller, M., Raschke, S., Friese, S., Ebert, F. and Schwerdtle, T. 2021, J. Trace. Elem. Med. Biol., 65, 126711.
27. Mohamed, A. S., Bin Dajem, S., Al-Kahtani, M., Ali, S. B., Alshehri, M., Shati, A., Morsy, K. and Fahmy, S. R. 2020, Bull. Environ. Contam. Toxicol., 105(6), 827-834.
28. Maluf, W., Filho, W., Parisotto, B., de Medeiros, G. d. S., Pereira, H. J., Maraslis, T., Schoeller, C. D., da Rosa, S. and Fröde, S. 2020, Genet. Mol., 43(2), 1-8.
29. Vogeler, S., Carboni, S., Li, X., Nevejan, N., Monaghan, S. J., Ireland, H. and Joyce, A. 2020, BMC Dev. Biol., 20(1), 23.
30. Canesi, L., Ciacci, C., Fabbri, R., Marcomini, A., Pojana, G. and Gallo, G. 2012, Mar. Environ. Res., 76, 16-21.